Pergamon

Journal of Structural Geology, Vol. 20, No. 8, pp. 1013 to 1022, 1998

0191-8141/98 $19.00 + 0.00

PII: S0191-8141(98)00030-3

The importance of overpressure timing and permeability evolution in fine-grained sediments undergoing shear

A. J. BOLTON and A. J. MALTMAN

Institute of Geography and Earth Sciences, University of Wales, Aberystwyth SY23 3DB, U.K.,
E-mail: aib94@aber.ac.uk

and

M. B. CLENNELL

Department of Earth Science, University of Leeds, Leeds LS2 9JT, U.K.

(*Received* 25 *July* 1997; *accepted in revised form* 22 *February* 1998)

Abstract—We summarise new experimental data which clarify the hydrological behaviour of clayey sediments undergoing shear, and which emphasise the importance of the relative timing of deformation and overpressure. Fluid flow in fine-grained materials subjected to shear is strongly dependent on the previous stress history of the material. Underconsolidated sediments, such as those that retain high porosities through retarded dewatering and consequent excess pore-fluid pressure generation, deform by bulk volume loss which reduces permeability. The deformation fabrics are pervasive in style, weakly developed, and without a significant influence on hydrological properties. In contrast, sediment that has been consolidated and then subjected to excess pore-fluid pressure deforms dilatively along discrete, brittle shear zones, which markedly affect the permeability. Moreover, below a certain threshold of effective stress, these localised zones prompt a markedly non-linear increase in hydraulic conductivity, a laboratory demonstration and quantification of the concept of fracture permeability. © 1998 Elsevier Science Ltd. All rights reserved

INTRODUCTION

Fluid pressure governs the strength and mechanical behaviour of sediments. Fine-grained sediments, the subject of this article, are particularly prone to develop overpressures (pore fluid pressures in excess of hydrostatic) because they commonly exhibit low permeabilities: the pore-fluids cannot escape at a rate commensurate with loading (basic terminology of sediment deformation and hydrology is reviewed in Maltman, 1995, chapters 1, 2 and 8). A well known example is the burial of shale in deltaic sequences such as those in the Gulf of Mexico (Harrison and Summa, 1991), where dewatering cannot keep pace with the rapid deposition of overlying sediments. Overpressures can also develop as a result of tectonic loading, for example through the partitioning of applied stresses into the pore fluid (Yassir and Bell, 1994). These processes are important in settings such as convergent plate margins, where fluid-rich sediment is subject to both gravitational compaction and tectonic shear (Moore *et al.*, 1991). The extent to which overpressures are dissipated or maintained is largely governed by the sediment's permeability (Magara, 1971; Mann and MacKenzie, 1990; Katsube *et al.*, 1991), and this is itself influenced by the deformation state of the material. It may well depend, for example, on whether the sediment is deforming by distributed ductile shear or in localised brittle shear zones.

We present here new laboratory data bearing on these matters. Our results highlight the importance of the previous effective-stress history of the sediment, particularly the consolidation state of the sediment at the onset of shear, for which overpressure timing is of particular importance. The data show that sediment which lies on the normal consolidation line (see Fig. 1 and the next section for further explanation), either through efficient dewatering during consolidation or retarded dewatering and development of early overpressure, behaves in a different manner during shear than material that has undergone consolidation and late overpressuring prior to deformation. Moreover, the hydrological behaviour following shear is influenced markedly by the deformation style that operated. We explore these concepts by firstly outlining a theoretical model that introduces the importance of overpressure timing, and then by reporting the laboratory tests that substantiate and extend the model. The interplay between permeability and timing of overpressure as illustrated by our data is relevant to several different geological environments. Both the sealing capacity of shales in petroleum systems and the dynamics of accretionary systems are highly dependent on the timing of fluid overpressure and the role of defor-

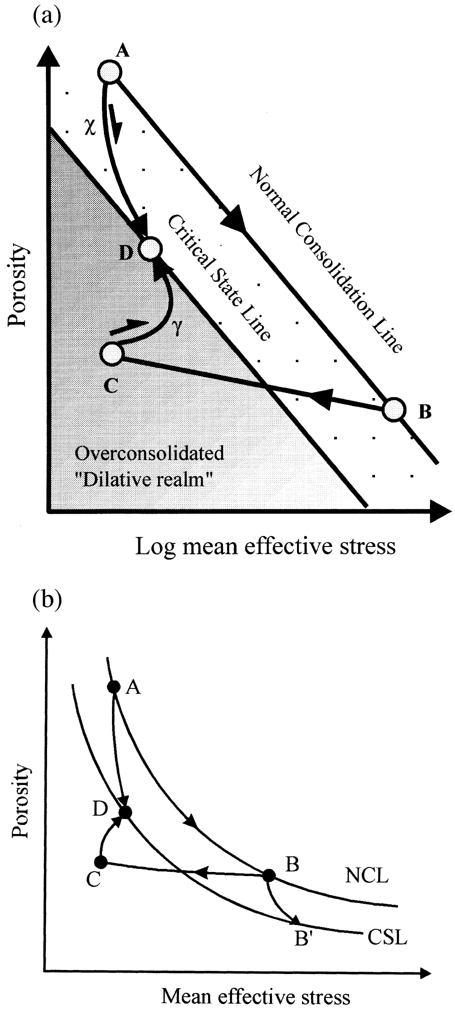

Fig. 1. (a) Theoretical stress paths for sediment that is deformed (line A–D), or consolidated (line A–B), unloaded by removal of overburden or increase in pore-fluid pressure (line B–C), and then sheared (line C–D). Note that sediment at identical effective stress (points A and C) may have markedly different porosity. Shear path χ indicates strain hardening and porosity collapse; shear path γ indicates strain hardening associated with dilation and subsequent softening. Shading emphasises that the boundary between different types of deformation mechanisms lie at the critical state line. (b) Diagrammatic representation of actual stress path for two samples plotted against porosity. Slurry consolidated along the normal consolidation line (line A–B). Normally consolidated sample then sheared along line B–B′. Note that sample loses volume to approach critical state. Overconsolidated sample unloaded first along line B–C (note the slight increase in porosity), before being sheared along line C–D. Sediment increases in porosity to approach critical state due to material lying below the critical state line at onset of shear. The lettering highlighting individual points is concordant with (a). Path A–D is shown as reference to that illustrated in theoretical model presented in (a).

mation fabrics in dictating the fluid transport properties of the host medium.

FLUID FLOW AND CONSOLIDATION

The governing equation for fluid flow in porous media known as Darcy's law relates the pressure head that sediment can sustain for a given rate of flow through the material. The ease with which flow moves through the pore space governs the magnitude and distribution of fluid pressures within the sediment. Given the close association between permeability and porosity, many workers have tried to attain a direct relation between the two parameters (e.g. Rogers *et al.*, 1995). However, the direct relationship still remains unclear. One particular reason for the discrepancy arises through the presence of a strong internal fabric, arising from reorientation of grains in response to burial or shear deformation. It is therefore not possible to be able to accurately determine the permeability of a sediment package from the porosity alone. This inference is largely supported by work conducted on sheared material, (Arch and Maltman, 1990; Brown and Moore, 1993; Brown *et al.*, 1994; Dewhurst *et al.*, 1996), where in all cases significant permeability anisotropy develops depending on the direction of flow relative to any deformation fabrics present. The mechanisms of permeability evolution during both burial, compaction and shear are all crucial to the development and subsequent dissipation of excess pore fluid pressures.

Widely used by engineers (Atkinson and Bransby, 1978; Lamb and Whitman, 1979), Terzaghi's theories of consolidation (porosity loss under load, Terzaghi, 1943; Taylor, 1948) have now been elaborated and applied to geological problems (Jones and Addis, 1986; Karig, 1990; Yassir, 1993). Sediment undergoing burial will follow a particular stress path that relates volume changes to imposition of load, depending on the rate of burial and also the material's permeability (Fig. 1a & b). For example, assuming efficient dewatering, increasing overburden will induce a reduction in porosity along the normal consolidation path A–B, presumably accompanied by a reduction in permeability. The gradient of the line reflects the compressibility of that sediment to changes in boundary stress conditions. Material cannot exist to the right of the normal consolidation line, and therefore the line represents a state boundary surface (Atkinson, 1993).

However, if dewatering is suppressed from the outset, the sediment will remain at point A, and the increased burial load will be partitioned into the pore-fluid, giving an increase in fluid pressure. High porosities will be maintained and the sediment becomes 'overpressured', a state often termed 'underconsolidated' (e.g. Rubey and Hubbert, 1959; Taylor and Leonard, 1990; Moore and Vrolijk, 1992). Note that the consolidation state of the material refers primarily to the magnitude of effective stress and not to the depth of burial. Furthermore, since the increasing load is supported by elevated fluid pressure, there is no change in effective stress and hence consolidation state (the sediment remains at point A on the normal consolidation line), even though the sediment is being increasingly buried.

Where the sediment has consolidated along path A–B, an ensuing reduction of effective stress moves it into the overconsolidated realm (path B–C). This state is marked by a slight increase in porosity, due to some elasticity in the sediment. Such a reduction in effective stress could arise through uplift and removal of overburden, or by injection or internal generation of pressurised fluids (such as water released by diagenetic transformation of smectite to illite, Bekins *et al.*, 1994) to give overpressuring. The magnitude of overpressuring will again depend on (among other factors) the material's permeability. This state is termed overconsolidation, and its magnitude can be defined by the overconsolidation ratio (OCR) which relates the maximum previous effective stress (p'_y) to the current stress acting upon the sediment (p'_0), such that,

$$\mathrm{OCR} = \frac{p'_y}{p'_0}.$$

It is therefore possible for sediment to have markedly different porosities but similar degrees of overpressuring, depending on the time at which the fluid pressures arise. Standard porosity–depth relationships (e.g. Athy, 1930; Magara, 1980) assume normal fluid pressures, and consequently any positive deviations away from the predicted profile are normally taken to indicate horizons of overpressure and underconsolidation (such as point A). However, horizons that have been subjected to late stage overpressuring (such as point C) will not demonstrate the same porosity anomaly because the bulk of the sediment is overconsolidated. That is, *the absence in a depth profile of a marked porosity deviation does not signify the absence of overpressured horizons*. The importance of this in deformation studies is that a sediment's response to shearing depends closely on the consolidation state of the material. Sediment will ultimately attempt to reach a 'critical state' during shear (Fig. 1a & b, and Atkinson and Bransby, 1978), in which strain accumulation occurs without an associated change in effective stress or volume. Normally consolidated and lightly overconsolidated sediments (normally those with an OCR of approximately less than 2, Wood, 1990) accommodate shear by bulk volume loss and ductile flow before achieving the critical state. This is due to the critical state line lying below the normal consolidation line. Conversely, heavily overconsolidated material ($\mathrm{OCR} > 2$) undergoes localised brittle failure (Skempton, 1966; Skempton and Petley, 1967) and associated volume increase (line C–D). Deformation is commonly associated with the development of discrete shear zones. The dilation that is necessary for shear zones to form is accompanied by a reduction in stiffness, and is therefore weaker than surrounding relatively undeformed sediment. Further straining is accommodated within the softer, dilating shear zone until critical state is reached. In this way, large shear strains can be achieved heterogeneously along extremely narrow discontinuities, while much of the surrounding sediment remains undeformed. Critical state will ultimately be reached within the individual shear bands. The interplay between consolidation, shear, permeability and overpressure is therefore a subtle one. We now report two series of laboratory experiments designed to explore and quantify some of the relationships.

EXPERIMENTAL METHODOLOGY

The two series of experiments were conducted on identical artificial samples made from a slurry of 80% kaolinite–20% fine sand sieved to $< 63\,\mu$m grain size and mixed with distilled water (see Maltman, 1987 for further methodological details). Figure 2(a & b) illustrates the stress paths followed by each sample. Both specimens were consolidated uniaxially to 500 kPa (path A–B, Fig. 2), trimmed to cylinders 38 mm diameter by 76 mm length, and mounted in a triaxial cell (path B–C). A 350 kPa back pressure saturated the sediment, and incremental increases of 50 kPa confin-

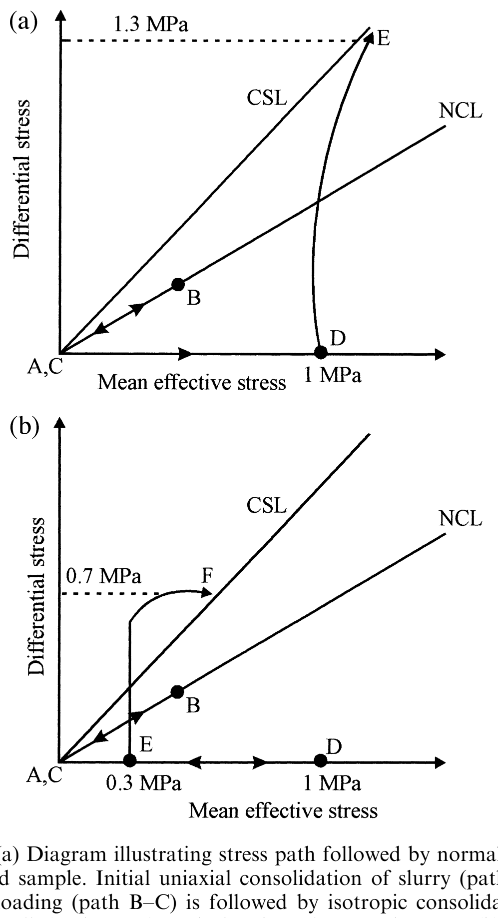

Fig. 2. (a) Diagram illustrating stress path followed by normally consolidated sample. Initial uniaxial consolidation of slurry (path A–B) and unloading (path B–C) is followed by isotropic consolidation in triaxial cell (path C–D) and shearing along path D–E. (b) Stress path summary for overconsolidated sample. Initial stress paths are identical as for normally consolidated sample shown in (a). After isotropic consolidation along path C–D, the mean effective stress is reduced to 0.3 MPa (path D–E), before shearing along line E–F.

ing pressure by using a GDS hydraulic actuator accurate to 1 kPa, led to a maximum effective isotropic consolidation stress of 1 MPa (path C–D). For each increment of consolidation, volume changes were monitored by measuring the outflow of water from the sediment.

One sample was then deformed axially at a constant strain rate and the axial stress monitored (path D–E, Fig. 2a). The strain rate was set at a minimum (2.85×10^{-7} s^{-1}) to ensure that deformation was fully drained (pore-fluid pressure able to dissipate during deformation). This meant that measured changes in the pore-fluid pressure were directly related to a modification of the sediment permeability. A second sample was consolidated similarly but deformed (along path E–F, Fig. 2b) after having been unloaded by a combination of reduced confining stress and increased pore-fluid pressure to an effective stress of 300 kPa (an overconsolidation ratio of 3.3, path D–E, Fig. 2b). It was deformed at the same strain rate as the earlier

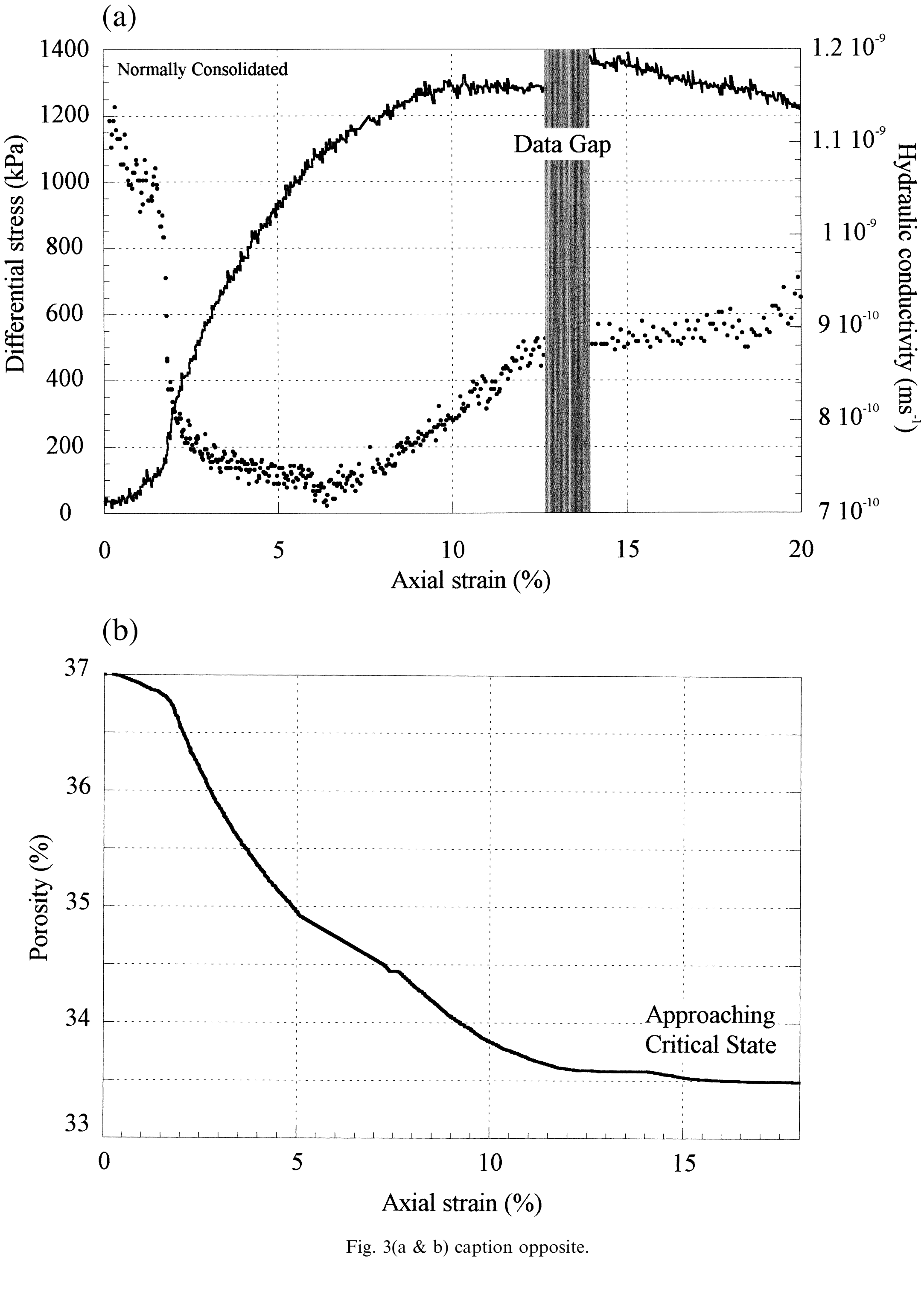

Fig. 3(a & b) caption opposite.

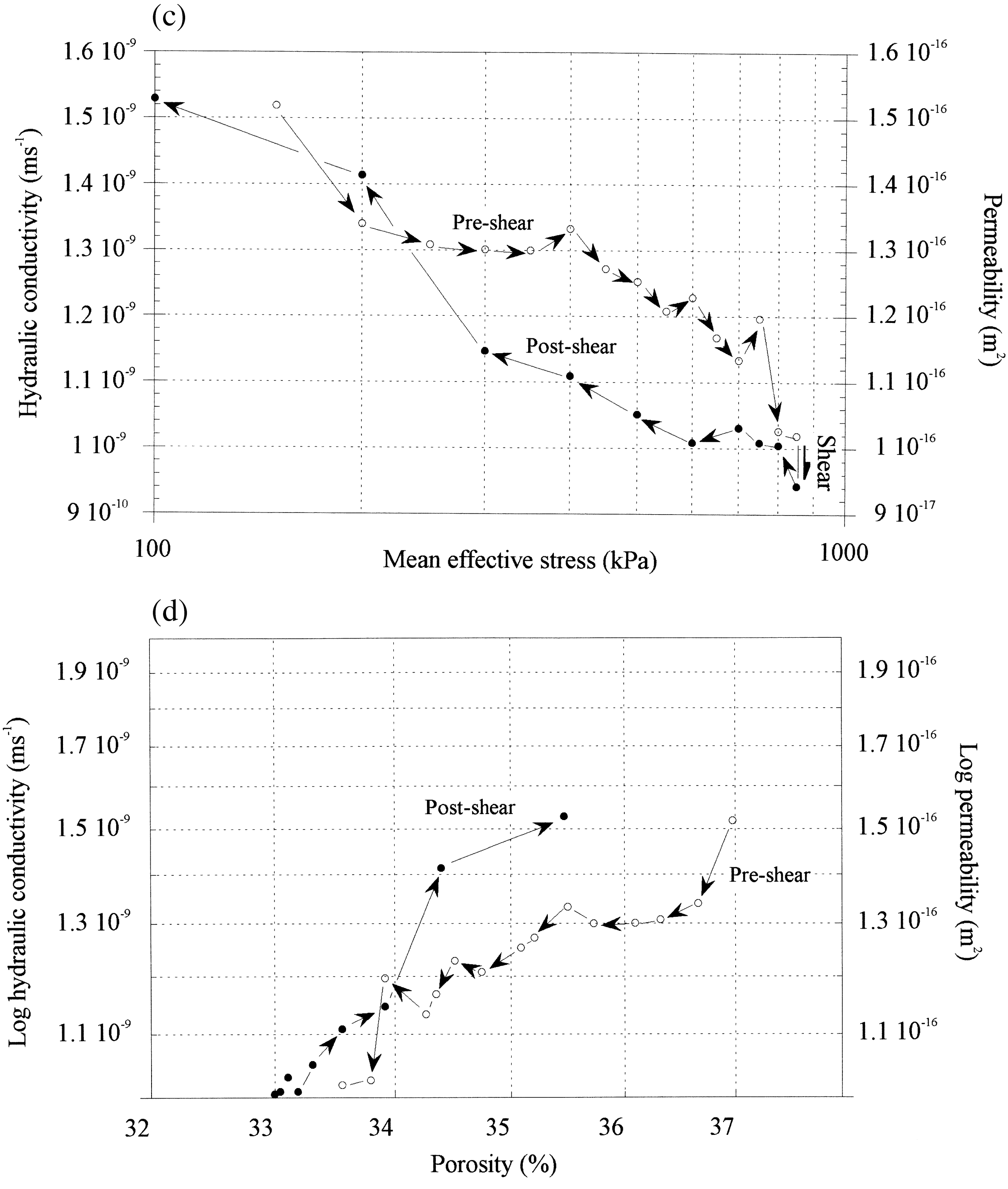

Fig. 3. (a) Differential stress and dynamic permeability (expressed as hydraulic conductivity) vs axial strain for normally consolidated sample. Differential stress represented by solid line, dynamic permeability by dots. (b) Bulk porosity evolution during shear of same normally consolidated sample. (c) Pre- and post-deformation hydraulic conductivity at different conditions of mean effective stress. Hollow circles are pre-shear, filled circles post-shear. Arrows indicate the increments of loading/unloading. Equivalent permeability values are represented on right hand *y*-axis. Lettering refers to sections indicated in text. (d) Log permeability vs porosity.

sample. Permeability was measured throughout the tests by a constant-rate-of-flow permeameter (Olsen, 1966; Aiban and Znidarcic, 1989). Permeant was introduced into the sample by a flow pump at a constant rate of 0.004 ml min^{-1}. The associated pressure head difference across the sample was monitored by a differential pressure transducer accurate to ± 1 kPa, from which the permeability was calculated in accordance with Darcy's law. The volume of permeant exiting the sample was monitored simultaneously by recording the pressure difference between the calibrated outflow burette and an air filled reference tube. By comparing the amount of fluid introduced into the top of the sample with the volume of fluid leaving the base of the sample volume changes could be calculated. Static permeability tests (where no axial load was applied) were terminated when a constant pressure head was measured and the volume of fluid infused and exiting from the sample were identical i.e. constant rate of flow was established. Permeability testing during shear (dynamic permeability measurement) was simultaneous with volume changes occurring, so flow was not strictly steady state. However, shearing was stopped periodically during deformation until steady state was achieved and the actual permeability measured before shearing was restarted. After cessation of shear, the post-deformation permeability of both samples was measured under various conditions of effective stress, by combinations of fluctuating confining pressure and pore-fluid pressure. Given the low permeabilities of these fine-grained materials, each suite of tests took about 2 months to complete. Note that the 'permeability' results below are presented as hydraulic conductivity, given that the permeant is pure water.

RESULTS AND DISCUSSION

The stress–strain and dynamic permeability behaviour (permeability during shear) of the normally consolidated sample is shown in Fig. 3(a). The sediment cylinder deformed by ductile barrelling, without developing discrete failure surfaces and without a well defined peak strength being evident on the stress–strain curve. The strain was accommodated by bulk volume loss (Fig. 3b), accounting for the overall drop in hydraulic conductivity. The small rise in hydraulic conductivity between 8% and 12% axial strain is contrary to what would be expected, given that the sediment is losing volume. However, decreasing the porosity will necessitate expulsion of fluid from the base of the sample. This removed fluid will increase the pressure at the downstream end, and hence the differential pressure will drop, creating the observed apparent increase in hydraulic conductivity. Post-shear hydraulic conductivity under varying conditions of effective stress indicates that any deformation fabrics that were produced had little influence on the fluid-flow (Fig. 3c). The permeability increased approximately along the expected log-linear swelling line, analogous to unsheared sediment on a decreasing effective stress path (Atkinson, 1993 and Fig. 3d).

Figure 4(a) shows the stress–strain and dynamic permeability behaviour of the overconsolidated sample. In contrast with the normally consolidated material, this sediment cylinder deformed along localised, inclined zones of shear rather than by overall barrelling. The failure surfaces paralleled each other at an angle of approximately 35° to the cylinder axis. The permeability increased with strain, as a result of dilation in the sample (Fig. 4b). The material displayed repeated strain hardening/strain softening events indicative of incremental stick-slip brittle failure. At each point of failure there was a minor drop in porosity and an associated fall in permeability. We interpret this to reflect collapse and locking of individual shear zones, creating an increase in sediment strength and therefore necessitating propagation of new zones into nearby undeformed areas.

We considered an alternative explanation, that water is being sucked into the dilating shear zones causing a drop in fluid pressure with no actual permeability change. Therefore, from time to time during the deformation, we temporarily halted the shear and measured the true, steady-state flow permeability. The values are equivalent to those measured during active shear, indicating that the variations of the pore-fluid pressure are due to changes in the fluid pathway, rather than transient pressure changes associated with movement of fluid into the dilating zones. The dilation occurring will cause fluid redistribution within the sediment. In other words, dilating shear zones will act as sinks for fluid, and cause a drop in fluid pressure. This will occur only if there is insufficient volume of fluid available to enter the zone of dilation. This effect is observed here, but the fact that the permeability does not change when shearing is temporarily ceased indicates first that the shear zones are interconnecting (with each other and to the base of the sample) and secondly that no creep occurs which would close up the dilated zone and reduce the permeability.

Our explanation that the effects are due to localised dilation within the evolving shear zones rather than to bulk dilation is supported by the results of Hicher *et al.* (1994). Using X-ray absorption, they observed that kaolin undergoing shear preferentially dilated within the shear zones and that bulk effects were negligible. It appears, therefore, that the main control on the hydrological properties of the sediment is the behaviour of the shear zones, and the influence of the bulk sediment is minimal.

The post-shear behaviour of the overconsolidated material is particularly significant. A permeability test was conducted with the differential stress still imparted on the sediment. This was then removed and another test conducted. There was no change in permeability, indicating that the effects of the differential stress are negligible, and the principal control on the permeability is the isostatic stress (confining and pore fluid pressure). This effective stress was first increased by raising the cell pressure to 800 kPa, and then reduced to 50 kPa through a combination of reduction of the confining pressure and increasing the pore fluid pressure. The relationships between porosity and permeability are markedly non-linear (Fig. 4c). The shallow linear loading curve with a porosity loss of 17 units with little change in permeability (path D–E on Fig. 4c) is likely to be concentrated within the more undeformed domains, since the shear zones assert a stronger influence on the hydrological properties of the sediment. Hence any matrix consolidation does not alter the permeability significantly. A highly inelastic response at increasing levels of pore-fluid pressure (the unloading path E–F on Fig. 4c) accounts for the marked lack of similarity between the loading and unloading curves.

However, the post-shear permeability depends primarily not on porosity but on effective stress (Fig. 4d). In contrast with the normally consolidated sample, the relationships are non-linear (path E–F on Fig. 4d) at low values of effective stress. Again, it seems that any matrix consolidation has little effect on the overall permeability and that the shear zones act as the main channels for fluid flow. This inference is borne from both the permeability during shear, and also the marked non-linearity of permeability after shear with effective stress. Indeed, at a certain threshold of decreasing effective stress (about 250 kPa for this ma-

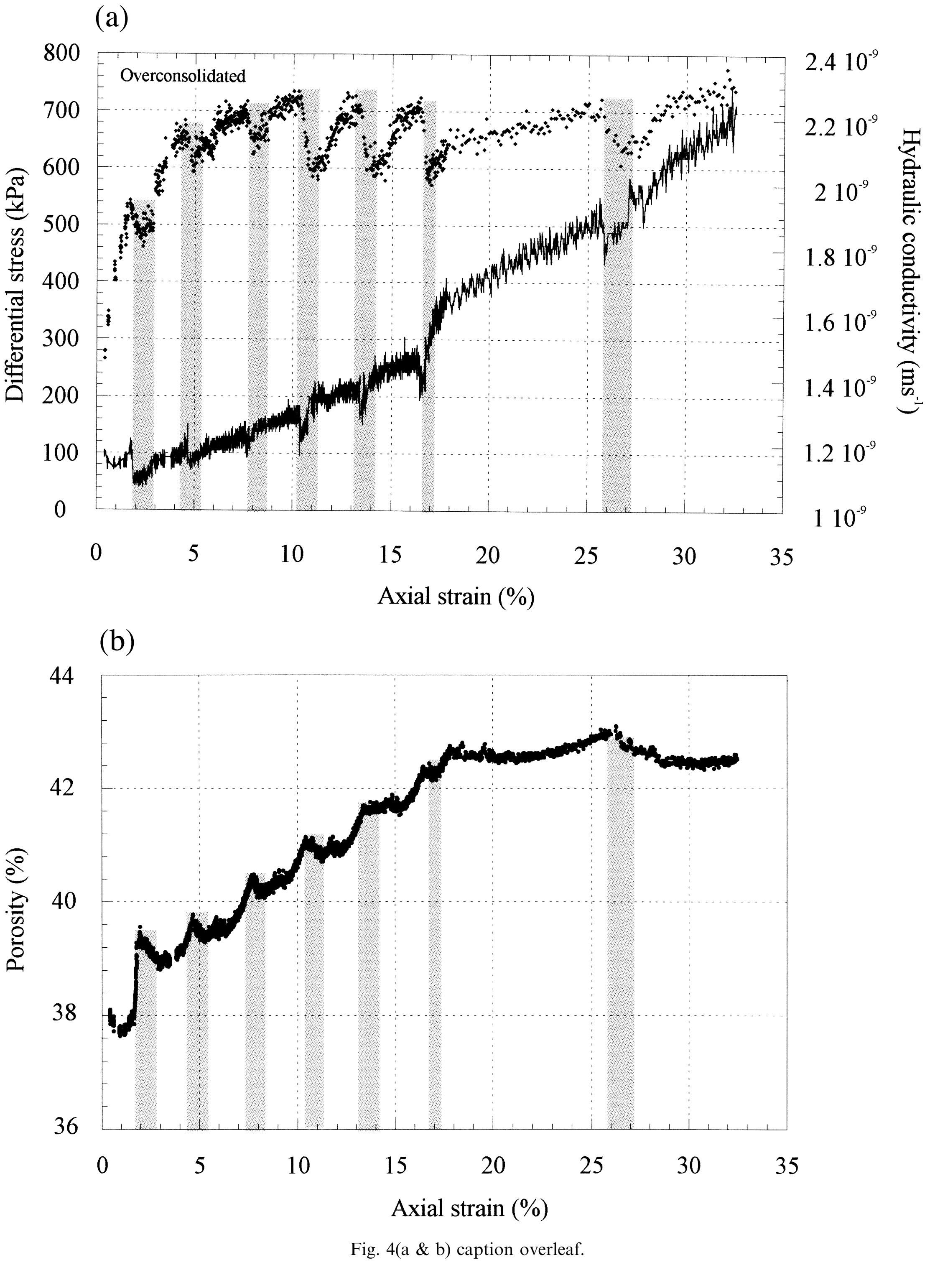

Fig. 4(a & b) caption overleaf.

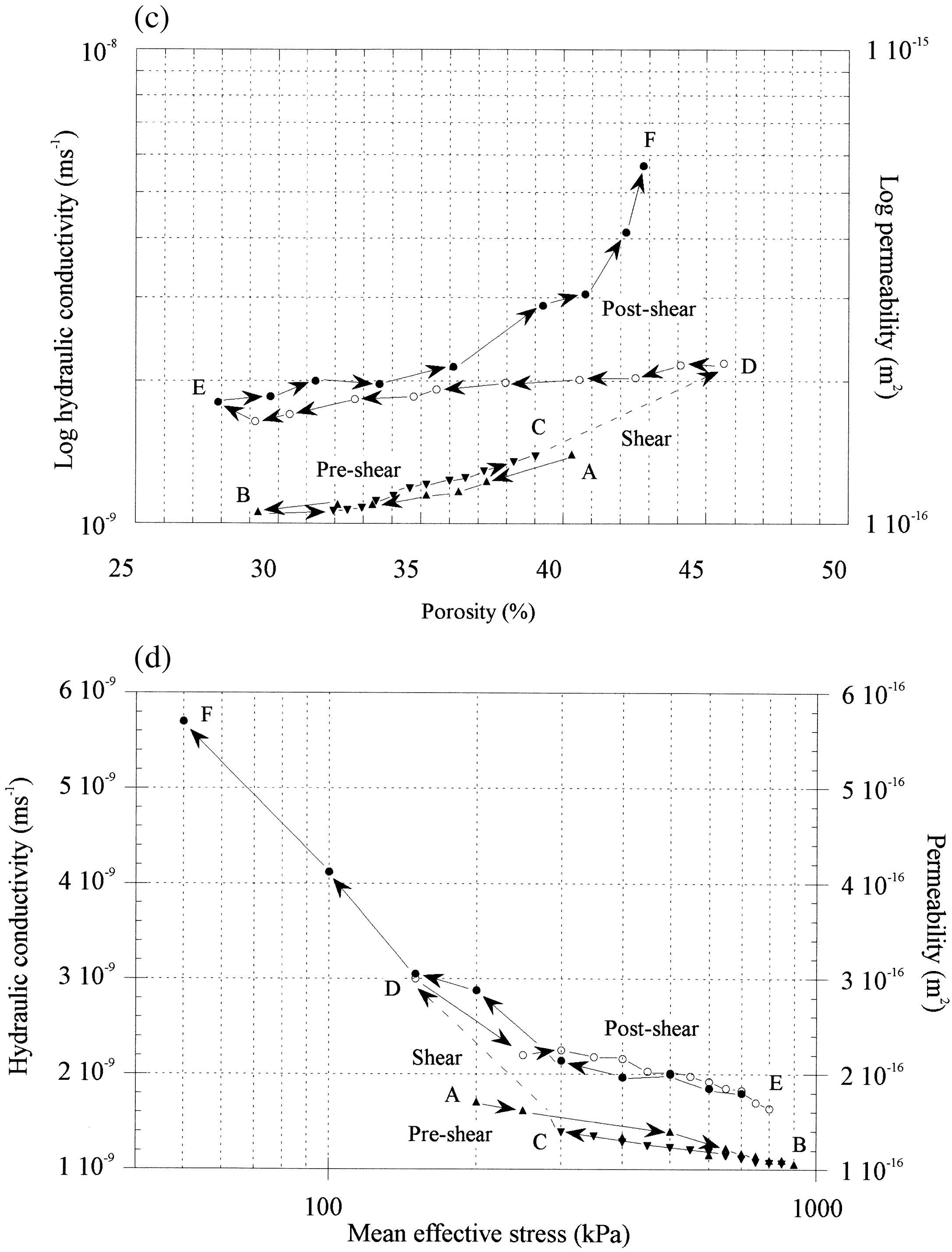

Fig. 4. (a) Differential stress and dynamic permeability vs axial strain for overconsolidated sample. Differential stress represented by diamonds, dynamic permeability by line. Shaded areas aid correlation between stress, permeability and porosity in (b). (b) Bulk porosity evolution during shear for same sample. Scales correspond with (a). (c) Permeability vs porosity relationship before and after shear. Triangles are pre-shear, dots are post shear. Arrows indicate direction of loading/unloading. Note non-linear relationship on unloading after shear. Lettering refers to sections indicated within the text. (d) Permeability vs mean effective stress relationship before and after shear.

terial), the shear zones start to connect and prompt a marked increase in permeability. Although the shear zone walls at this stage are parting due to the reduction in effective stress, the small amount of porosity increase is sufficient to create a more interconnected pathway, and hence the permeability increases more than would be expected. Such a concept has been referred to as 'fracture permeability' (e.g. Gutfraind and Hansen, 1995). Whether the shear zones are actually dilated fractures or cohesive intact zones is unclear, but the results are consistent with other laboratory evidence that sheared fine-grained sediments enhance flow (Arch and Maltman, 1990).

Limitations of the triaxial arrangement do not allow strains greater than about 35%, which may explain why residual state was never reached in the experiments. Similar studies conducted with a ring shear apparatus (Brown *et al.*, 1994; Dewhurst *et al.*, 1996) in which the material can be deformed to very much larger strains, show that a large permeability anisotropy develops due to shear zone development, but is associated with an overall decrease in permeability. Thus, the data presented here may be a demonstration of how shear zones become transient flow conduits during the early stages of deformation, before larger strains induce porosity collapse and permeability reduction as the material approaches critical state. However, if stick-slip deformation is the dominant mechanism of shear, then although large shear strains may develop cumulatively, the actual amount of shear strain taken up on individual surfaces will be relatively small. In this way, the sediment may never reach critical state.

CONCLUSIONS

The behaviour of sediment in shear is highly dependent on its hydrological properties, which interact with the effective stress history of the material. Our experiments show that although elevated pore-fluid pressures reduce effective stress and enhance shear deformation, the consolidation state at the onset of shear is a crucial factor on the deformation style and the resultant permeability. Therefore, when considering how overpressured sediments behave during shear, it is the timing of overpressure which is particularly relevant, as this can change the consolidation state with respect to effective stress. Sediment lying on the normal consolidation (arising through either inefficient dewatering as indicated in Fig. 1a, or by full consolidation as presented in the data) will deform by ductile mechanisms and undergo an overall reduction in permeability during later shear. Localised flow will tend not to occur. In contrast, overpressuring that arises after burial induces overconsolidation. Our data suggest that shear strain is accommodated by brittle stick-slip dilational failure along discrete shear horizons and these act as conduits. There are some increases in permeability during shear-zone propagation and small reductions when pores within the zones collapse.

In deformed overconsolidated sediment, reductions in effective stress give small increases in porosity and associated permeability through elastic swelling of the sediment, until a threshold point is reached. Below this, the low effective stresses allow zones of aligned grains to open progressively and act as conduits for fluid flow. The concept has been referred to as 'fracture permeability'. We believe that our experiments have provided evidence supporting the existence of this mechanism and have begun to quantify the physical conditions in which this potentially important dewatering process can operate.

Acknowledgements—Harold Tobin and Julia Morgan are thanked for their detailed reviews which greatly improved the manuscript. Malcolm Peters is acknowledged for many stimulating discussions regarding fluid flow in deforming sediments. Aisling Broderick is also thanked for reading the manuscript. The research is supported by grant GT4/94/914/G from the Natural Environmental Research Council.

REFERENCES

Arch, J. and Maltman, A. J. (1990) Anisotropic permeability and tortuosity in deformed wet sediments. *Journal of Geophysical Research* **95,** 9035–9046.

Athy, L. F. (1930) Density, porosity and compaction of sedimentary rocks. *Bulletin of the American Association of Petroleum Geologists* **14,** 1–24.

Aiban, S. and Znidarcic, D. (1989) Evaluation of the flow pump and constant head techniques for permeability measurement. *Géotechnique* **45,** 69–81.

Atkinson, J. H. (1993) *An Introduction to the Mechanics of Soils and Foundations*. McGraw-Hill, London.

Atkinson, J. H. and Bransby, P. L. (1978) *The Mechanics of Soils: An Introduction to Critical State Soil Mechanics*. McGraw-Hill, London.

Bekins, B., McCaffrey, A. M. and Dreiss, S. J. (1994) Influence of kinetics on the smectite to illite transition in the Barbados accretionary prism. *Journal of Geophysical Research* **99,** 18,147–18,158.

Brown, K. M. and Moore, J. C. (1993) Comment on "Anisotropic Permeability and Tortuosity in Deformed Wet Sediments" by J. Arch and A. Maltman. *Journal of Geophysical Research* **98,** 17,859–17,864.

Brown, K. M., Bekins, B., Clennell, M. B., Dewhurst, D. and Westbrook, G. (1994) Heterogeneous hydrofracture development and accretionary fault dynamics. *Geology* **22,** 259–262.

Dewhurst, D., Clennell, M. B., Brown, K. M. and Westbrook, G. (1996) Fabric and hydraulic conductivity of sheared clays. *Géotechnique* **46,** 761–768.

Gutfraind, R. and Hansen, A. (1995) Study of fracture permeability using the Lattice-Gas automata. *Transport in Porous Media* **18,** 131–149.

Harrison, W. J. and Summa, L. L. (1991) Paleohydrogeology of the Gulf of Mexico basin. *American Journal of Science* **291,** 109–176.

Hicher, P. Y., Wahyudi, H. and Tessier, D. (1994) Microstructural analysis of strain localisation in clay. *Computers and Geotechnics* **16,** 205–222.

Jones, M. E. and Addis, M. A. (1986) The application of stress path and critical state analysis to sediment deformation. *Journal of Structural Geology* **8,** 575–580.

Karig, D. E. (1990) Experimental and observational constraints on the mechanical behaviour in the toes of accretionary prisms. In *Deformation Mechanisms, Rheology and Tectonics*, ed. R. J. Knipe and E. H. Rutter, pp. 383–398. Geological Society of London. Special Publications **54**.

Katsube, T. J., Mudford, B. S. and Best, M. E. (1991) Petrophysical characteristics of shales from the Scotian Shelf. *Geophysics* **56,** 1681–1689.

Lamb, T. W. and Whitman, R. V. (1979) *Soil Mechanics, S. I. Version*, 2nd edn. Wiley, New York.

Magara, K. (1971) Permeability considerations in the generation of abnormal pressures. *Journal of the Society of Petroleum Engineers Paper* **11,** 236–242.

Magara, K. (1980) Comparison of porosity-depth relationship of shale and sandstone. *Journal of Petroleum Geologists* **3,** 175–185.

Maltman, A. J. (1987) A laboratory technique for investigating the deformation microstructures in water-rich sediments. In *Deformation of Sediments and Sedimentary Rocks*, ed. M. E. Jones and R. M. F. Preston, pp. 71–76. Geological Society of London. Special Publications **29**.

Maltman, A. J. (1995) *The Geological Deformation of Sediments*. Chapman & Hall, London.

Mann, D. M. and MacKenzie, A. A. (1990) Prediction of pore fluid pressures in sedimentary basins. *Marine and Petroleum Geology* **7,** 55–68.

Moore, J. C., Brown, K. M., Horath, F., Cochrane, G., MacKay, M. and Moore, G. (1991) Plumbing accretionary prisms: effects of permeability variations. *Philosophical Transactions of the Royal Society of London* **335,** 275–288.

Moore, J. C. and Vrolijk, P. (1992) Fluids in accretionary prisms. *Reviews of Geophysics* **30,** 113–135.

Olsen, H. W. (1966) Darcy's law in saturated kaolinite. *Water Resources Research* **2,** 287–295.

Rogers, S. J., Chen, H. C., Kopaskamerkel, D. C. and Fang, J. H. (1995) Predicting permeability from porosity using artificial neural networks. *Bulletin of the American Association of Petroleum Geologists* **79,** 1786–1797.

Rubey, W. and Hubbert, M. (1959) Role of fluid pressure in overthrust faulting: II. Overthrust belt in a geosynclinal area of western Wyoming in the light of the fluid pressure hypothesis. *Bulletin of the American Association of Petroleum Geologists* **70,** 167–207.

Skempton, A. W. (1966) Some observations of tectonic shear zones. *Proceedings of the First International Conference on Rock Mechanics, Lisbon* **6,** 329–335.

Skempton, A. W. and Petley, D. (1967) Strength along structural discontinuities in stiff, fissured clay. *Proceedings of the Oslo Geotechnical Conference* **2,** 2–30.

Taylor, D. W. 1948. *Fundamentals of Soil Mechanics*, Wiley, New York.

Taylor, E. and Leonard, J. (1990) Sediment consolidation and permeability at the Barbados Forearc. In *Proceedings of the Ocean Drilling Program, Scientific Results*, eds J. C. Moore, A. Mascle, E. Taylor and M. B. Underwood, **110,** pp. 97–110.

Terzaghi, K. (1943) *Theoretical Soil Mechanics*. Wiley, New York.

Wood, D. M. (1990) *Soil Behaviour and Critical State Soil Mechanics*, 1st edn. Cambridge University Press, Cambridge.

Yassir, N. A. (1993) Over-pressures, fluid flow and stress regimes in the Jeanne d'Arc basin. *Canada International Journal of Rock Mechanics, Mineral Science and Geomechanical Abstracts* **30,** 1209–1213.

Yassir, N. A. and Bell, J. S. (1994) Relationships between pore pressure, stresses, and present day geodynamics in the Scotian shelf, offshore eastern Canada. *Bulletin of the American Association of Petroleum Geologists* **78,** 1863–1880.